ANALYSIS AND DETECTION OF MOTION ARTIFACT IN PHOTOPLETHYSMOGRAPHIC DATA USING HIGHER ORDER STATISTICS

Rajet Krishnan, Balasubramaniam Natarajan and Steve Warren

Department of Electrical and Computer Engineering,
Kansas State University, Manhattan, Kansas 66506-5204

ABSTRACT

In this work, we present novel methods for detecting the presence of motion artifact in photoplethysmographic (PPG) measurements based on higher order statistical information present in the data. We analyze both clean and corrupt PPG data in the time and frequency domains. In the time domain, skew and kurtosis measures of the signal are used as distinguishing metrics between clean and motion-corrupted data. In the frequency domain, the presence of random components due to motion artifact is analyzed using a frequency domain kurtosis measure. Additionally, bispectral analysis of PPG data indicates the presence of strong quadratic phase coupling (QPC) and more specifically self coupling in the case of clean PPG data. Though quadratic phase coupling is found in data corrupted by motion artifact, the self coupling feature is absent. A Neyman-Pearson (NP) detection rule is formulated for each of the measures. Additionally, treating each of the measures as observations from independent sensors, the Varshney-Chair rule [11] is used to fuse individual decisions to form a global system decision.

Index Terms— Higher Order Statistics (HOS), Quadratic Phase Coupling (QPC), Receiver Operating Characteristics (ROC)

1. INTRODUCTION

Corruption of PPG measurements by motion artifacts has been a significant obstruction to the efficient and reliable use of pulse oximeters for continuous real-time health monitoring [8]. Motion artifact that mixes with the desired data resides in the same frequency range as that of the data (2-5 Hz). Over the years, many researchers have focused their efforts on motion artifact removal techniques. While removing motion artifact is critical, *detecting its presence is a key task that needs to be addressed first*. A reliable motion artifact detection technique lays the foundation for a completely automated PPG data processing system that identifies PPG data frames that are corrupted with artifacts and further processes them for motion artifact removal. Some work has addressed the detection issue by correlating a PPG data frame with a clean reference signal to detect motion artifact [12]. However, such techniques are unsuitable for robust continuous real-time monitoring.

This work addresses the issue of detecting the presence of motion artifact based on the inherent characteristics of PPG data. Specifically, the HOS properties of clean and motion corrupted PPG data are used as distinguishing features to aid detection. HOS properties have been investigated in the context of other biomedical signals [1]. Fourth order cumulants were used in [2] to dynamically determine rhythmic oscillations in PPG data. However, we believe that the work presented here is the first effort to employ HOS analysis for motion detection in PPG data.

We first analyze the PPG data from different subjects in both the time and frequency domains. In the time domain, skew and kurtosis measures associated with the data are analyzed. In the frequency domain, the presence of random components due to motion artifact is ascertained using a frequency-domain kurtosis measure as in [9]. Furthermore, bispectral analysis of PPG data indicates the presence of strong quadratic phase coupling (QPC) and more specifically self coupling in the case of clean PPG data. In motion artifact corrupted data, QPC between random frequency components is observed, but the self coupling feature is absent. Neyman Pearson (NP) tests are formulated based on the time domain and frequency domain metrics mentioned. Using practical test data, we characterize the performance (probability of false alarm-P_F, probability of detection-P_D, probability of error-P_{error}) of the detection tests. The performance results illustrate the potency of the proposed methodology for consistent and robust detection of motion artifact in PPG data.

The paper is organized as follows. The theory of HOS measures considered in this work is briefly discussed in 2. The results of PPG data analyses (with and without motion artifact) based on the above measures are presented in section 3. Based on these results, a Neyman-Pearson detection (NP) rule is formulated for each of the measures and discussed in section 4. Section 5 addresses the combination of all of these measures to formulate overall system decision. We conclude the paper in section 6.

2. THEORY

The HOS measures considered in this work follow:

1. *Skew and Kurtosis* - The skew and kurtosis of a random variable X is given by

$$\begin{aligned} C_{3x}(0,0) &= \frac{\mu_3}{\sigma^{3/2}} \quad \text{(skew)} \\ C_{4x}(0,0,0) &= \frac{\mu_4}{\sigma^4} - 3 \quad \text{(kurtosis)} \end{aligned} \tag{1}$$

   where σ is the standard deviation; μ_3 and μ_4 are the third and fourth moments, respectively. Skew is a measure of the symmetry (or the lack of it) of a probability distribution, while the kurtosis measure indicates a heavy tail and peakedness *OR* a light tail and flatness of a distribution relative to the normal distribution. This measure captures the random variations of data from the mean.

2. *Bispectrum* - The third-order polyspectrum of a random variable X is defined as the Fourier transform of its third cumulant

sequence -

$$S_{3x}(f_1, f_2) = \sum_{k=-\infty}^{\infty} \sum_{l=-\infty}^{\infty} [C_{3x}(k,l) \exp(-j2\pi(f_1 k + f_2 l))]$$

where $C_{3x}(k,l)$ is the third cumulant sequence of X. The power spectrum suppresses all phase information in a random process, while the bispectrum does not. When the harmonic components of a process interact, in addition to the contribution of power at their sum and difference frequencies, definitive phase relations also exist; this is called *Quadratic Phase Coupling* (QPC). For example, consider the following process:

$$X_1(k) = \cos(\lambda_1 k + \phi_1) + \cos(\lambda_2 k + \phi_2) + \cos(\lambda_3 k + \phi_3) \quad (2)$$

where $\lambda_3 = \lambda_1 + \lambda_2$, indicating that λ_1, λ_2 and λ_3 are harmonically related. If ϕ_1, ϕ_2 and ϕ_3 in (2) are independent random variables uniformly distributed in the range [0,2π], then (λ_3, ϕ_3) is an independent harmonic component. However, if in (2), $\phi_3 = \phi_1 + \phi_2$, then (λ_3, ϕ_3) is the result of quadratic coupling between (λ_1, ϕ_1) and (λ_2, ϕ_2). A detailed comprehensive treatment of topics pertaining to HOS can be found in [3]-[7]

3. DATA ANALYSIS

Analysis of PPG data is performed in order to understand and extract features that can be used as distinguishing metrics between clean and motion corrupted data. Data are collected using a reflectance pulse oximeter [8] from two healthy subjects in the age group of 22-24 years. The subjects follow the same motion patterns as in [8]:

1. Stationary Position: The subjects are required to be perfectly still - no movement of the wrist, fingers and elbow.
2. Finger movements (three cases): left-right (swinging), up-down (bending), and arbitrary finger movements. These are performed keeping the wrist and elbow stationary.
3. Wrist movements: The wrist is rotated and arbitrarily moved, keeping the elbow and fingers stationary.
4. Elbow movements: The elbow is bent and stretched, keeping the wrist and the fingers stationary.

Data are fed into a MATLAB script that dissects the entire data segment into short frames of equal length. First, each of the segments are passed through a bandpass filter (0.3-12 Hz). Here, the design of the filter is critical as the phase information in the data needs to be preserved in order to retain the shape of the PPG waveform. For this purpose, a zero-phase forward-reverse filter of order four in both directions is chosen. After filtering, the trend associated with each data segment is removed by extracting an appropriately fitted polynomial curve. Each frame of data is then inspected in the time and frequency domains, and the HOS properties are characterized.

3.1. Time Domain Analysis

In the time domain, we analyze the skew and kurtosis measure of the time variation of the PPG signal in each frame considered. This is done by evaluating equation (1) for each data frame. It is, however, important to note that these measures will vary with age and health condition. It is observed that the skew and kurtosis measured for the case of motion corrupt data is *much higher in magnitude* when compared to clean data. Therefore, these measures serve as features for motion detection.

3.2. Frequency Domain Analysis

In the frequency domain, the kurtosis measure is computed for the magnitude of the Fourier spectrum for each data frame. This measure considers the magnitude of the components present at each frequency sampled by the Discrete Fourier Transform (DFT) operation. It is seen that kurtosis is lesser in magnitude for frames corrupted with motion artifact when compared to those with clean data. This means a Fourier spectrum of clean data has a lesser number of significant frequency components (since only the harmonic components are prominent) compared to a spectrum of motion corrupted data (that consists of random spectral components).

3.3. Bispectral Analysis and Quadratic Phase Coupling

The bispectrum and the bicoherence of the data frames are analyzed using the MATLAB Higher-Order Spectral Analysis Toolbox [5]. Significant peaks at non-zero frequencies are observed in the bispectrum diagonal slice plots for clean PPG data, thereby confirming the presence of strong quadratic phase coupling. The diagonal slice plot indicates the frequencies that are being significantly coupled. In the case of clean PPG data, Table 1 indicates peaks at kf_0 Hz, $k = 1, 2, 3$, where $f_0 = 1.54$ Hz is the most dominant frequency being coupled, indicating the presence of *self coupling* between frequencies (we have $f_0 + f_0 = 2f_0$ and $f_0 + 2f_0 = 3f_0$ and so on, indicating the peaks in the diagonal slice plot). However, in the case of corrupt PPG data, QPC is observed to occur between random frequency components and the phenomenon of *self coupling* is absent as shown in Table 2. The features used for motion detection are summarized below:

1. *Time-Domain Features*: Skew and kurtosis measures that provide information on the distribution of data. They contain information regarding the shape of the PPG waveform.
2. *Frequency-Domain Feature*: Frequency domain kurtosis measure that indicates the presence of random components in the Fourier spectrum, thereby differentiating the spectrum of a clean signal that contains only the main harmonics.
3. *Bispectral Feature and Quadratic Phase Coupling*: Clean PPG data are characterized by the presence of strong *self coupling*

Table 1. Bispectrum Plot Results - Clean Data

Coupling Frequency (f) Hz	Coupling Magnitude
1.54	0.1565
3.08	0.0211
4.62	0.0037

Table 2. Bispectrum Plot Results - Corrupt Data

Coupling Frequency (f) Hz	Coupling Magnitude
0.74	0.2839
2.74	0.0081
4.41	0.0009

between the fundamental components of the frequency spectrum. This is absent in artifact corrupt measurements where quadratic phase coupling between random frequency components is observed.

4. DETECTION TEST

NP Detection Rule Formulation: PPG data are collected from 10 healthy subjects, both male and female, in the age group of 22-30 years (different subjects from those considered for analysis and feature extraction in section 3), in order to formulate the hypotheses for NP detection rule. They follow the same motion routines as detailed in section 3. Based on data obtained, the distinguishing measures are computed for each data frame as described in section 3. For each of the measures, let H_0 denote the null hypothesis corresponding to the region for clean data and H_1 denote the alternative hypothesis corresponding to the region for corrupt data. Under the hypotheses H_0 and H_1 the time-domain kurtosis, skew measures and frequency domain kurtosis measures are distributed as

$$\begin{aligned} H_0: &\quad y_i \sim \mathcal{N}(\mu_{0i}, \sigma_{0i}^2) \\ H_1: &\quad y_i \sim \mathcal{N}(\mu_{1i}, \sigma_{1i}^2) \qquad \forall i \in \{1,2,3\} \end{aligned} \tag{3}$$

where $\mathcal{N}(\mu, \sigma^2)$ is a Gaussian distribution with mean μ and variance σ^2; i corresponds to each of the distinguishing metrics. y_i is the observation based on time-domain kurtosis ($i = 1$), skew ($i = 2$) and frequency domain kurtosis ($i = 3$) measures. Based on values of the time-domain kurtosis and skew for each frame, local decisions $\delta_i \in \{0, 1\}$ are made according to

$$\delta_i = \begin{cases} 1 & \text{if } y_i \geq \eta_i \\ 0 & \text{if } y_i < \eta_i \end{cases} \qquad \text{for } i \in \{1,2\} \tag{4}$$

where $\eta_i = \sigma_{0i}\mathcal{Q}^{-1}(1 - P_{F_i}) + \mu_{0i}$, $\delta_i = 0$ corresponds to the null hypothesis, and $\delta_i = 1$ corresponds to the alternative hypothesis. Here P_{F_i} is the false-alarm probability, P_{D_i} is the corresponding probability of detection for each measure, and $\mathcal{Q}^{-1}$ is the inverse $\mathcal{Q}$-function. For frequency domain kurtosis, a decision is made according to

$$\delta_i = \begin{cases} 1 & \text{if } y_i \leq \eta_i \\ 0 & \text{if } y_i > \eta_i \end{cases} \qquad \text{for } i = 3 \tag{5}$$

where $\eta_i = \sigma_{0i}\mathcal{Q}^{-1}(P_{F_i}) + \mu_{0i}$. It can be easily shown for the time-domain kurtosis and skew measures that

$$\begin{aligned} P_{F_i} &= 1 - \mathcal{Q}\left(\frac{\eta_i - \mu_{0i}}{\sigma_{0i}}\right) \text{ and} \\ P_{D_i} &= 1 - \mathcal{Q}\left(\frac{\eta_i - \mu_{1i}}{\sigma_{1i}}\right). \end{aligned} \tag{6}$$

For the frequency domain kurtosis measure, the corresponding P_{F_i} and P_{D_i} are given by

$$\begin{aligned} P_{F_i} &= \mathcal{Q}\left(\frac{\eta_i - \mu_{0i}}{\sigma_{0i}}\right) \text{ and} \\ P_{D_i} &= \mathcal{Q}\left(\frac{\eta_i - \mu_{1i}}{\sigma_{1i}}\right). \end{aligned} \tag{7}$$

The tests in (4) and (5) are applied to data obtained from three healthy test subjects of 22-30 years (different subjects from those considered for formulating hypotheses in (3)). The performance of the detectors on test data and theoretical receiver operating characteristics (ROC) for the tests are shown in Figure 1. It is important to note that the performance on test data conforms to that expected in theory, assuming a Gaussian distribution for y_i. The kurtosis measures in the time and frequency domains are better in performance compared to the skew measure in the time domain. This is because the skew measure indicates the symmetry (or the lack of it) of the distribution of the data about the mean and is thus more characteristic of the PPG waveform (or the subject), while the kurtosis measure captures random variations from the mean.

Self Coupling Detection Rule: As concluded earlier, clean PPG data are characterized by self coupling, which is absent from data containing motion artifact (though QPC between random frequency components is present). That is, self coupling implies that the data are clean. Hence, to determine the presence/absence of self coupling, the frequencies being coupled are noted for each data frame and a decision is made as follows:

$$\delta_i = \begin{cases} 1 & \text{Self coupling} \Rightarrow \text{clean data} \\ 0 & \text{No self coupling} \Rightarrow \text{corrupt data} \end{cases} \tag{8}$$

The P_D and P_F measures related to the self coupling measure are directly computed from the initial training set. The P_F value is found to be 0.0420, while the P_D value is found to be 0.8932.

5. DECISION FUSION

The time domain measures (kurtosis, skew) and the frequency domain measures (QPC, kurtosis) are modeled as four individual sensors whose independent decisions can be fused to detect the presence of motion artifact in a given data frame. To implement this sensor fusion, the Varshney-Chair rule [11] is used. The work describes a rule that fuses individual sensor decisions while minimizing the probability of error of the overall detection system. Weights or reliability measures that are a function of individual P_{F_i} and P_{D_i} are associated with the decisions made by the individual sensors, and the fused global decision is given as follows:

$$f(\delta_1, \ldots, \delta_n) = \begin{cases} +1 & \text{if } a_0 + \sum_{i=1}^{4} a_i \delta_i > 0 \\ -1 & \text{otherwise,} \end{cases} \tag{9}$$

where $\delta_i = +1$ and $\delta_i = -1$ $\forall i \in \{1,2,3,4\}$ are the decisions made by the individual sensors corresponding to the presence/absence of motion artifact respectively based on the detection rules developed in section 4. The weights a_i are defined as

$$a_0 = 0 \tag{10}$$

$$a_i = \log\left(\frac{P_{D_i}}{P_{F_i}}\right) \text{ if } \delta_i = +1 \tag{11}$$

$$a_i = \log\left(\frac{1 - P_{F_i}}{1 - P_{D_i}}\right) \text{ if } \delta_i = -1 \tag{12}$$

assuming uniform cost assignment and equal prior probabilities for both hypotheses in (3).

The tests in (4), (5) and (8) are applied to data obtained from three test subjects as described in the previous section to obtain δ_i $\forall i \in \{1,2,3,4\}$. We select thresholds in (4) and (5) to yield a $P_{F_i} = 0.2$. We then evaluate the individual P_{D_i} followed by their respective P_{error}. Using this, the weights are computed in (10) and the fused decision is formed using (9). This is repeated for $P_{F_i} = 0.4$. The results are summarized in Table 3. It can be easily seen that in both the cases of P_{F_i}, the fused decision provides a better probability of detection of motion artifact than the individual sensors.

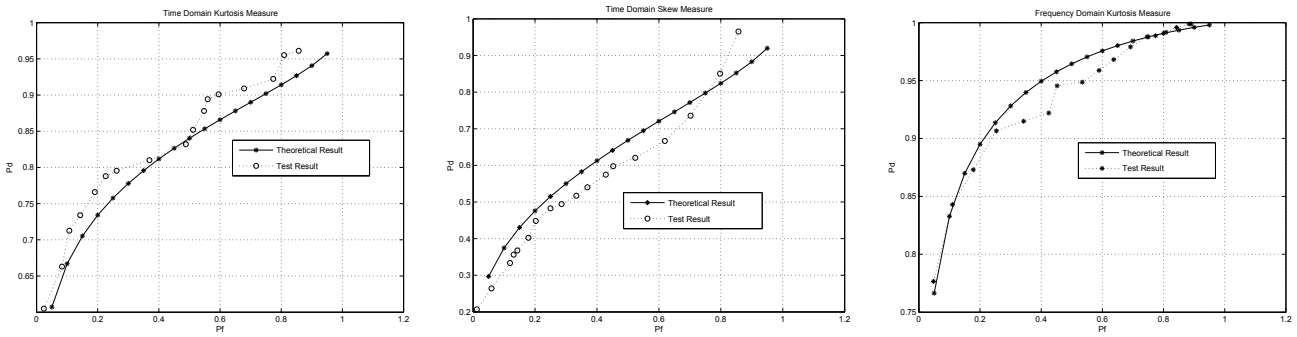

(a) (b) (c)

Fig. 1. Receiver Operating Characteristic (ROC) for a) Time domain kurtosis measure. (b) Time domain kurtosis measure. (c) Frequency domain kurtosis measure.

Table 3. Sensor Decision Fusion Results

Sensor	P_F	P_D	P_{error}	P_F	P_D	P_{error}
Kurtosis	0.2	0.78	0.16	0.4	0.85	0.19
Skew	0.2	0.42	0.40	0.4	0.58	0.47
QPC	0.04	0.89	0.08	0.04	0.89	0.08
FDK	0.2	0.9	0.2	0.4	0.92	0.25
Fused Decision	0.06	0.91	0.07	0.2	0.97	0.11

6. CONCLUSIONS

In this paper, we present a novel method for detection of motion artifact in PPG data, primarily considering higher order statistics (HOS) information present in the data. In the time domain, we observe that the skew and kurtosis measures associated with the corrupt PPG data are much higher in magnitude when compared to clean PPG data. The frequency-domain kurtosis measure is much smaller for the corrupt data frames than the clean ones. Bispectral analysis of PPG data indicates the presence of strong quadratic phase coupling (QPC) and, more specifically, self-coupling in the case of clean PPG data. Though quadratic phase coupling is found in data corrupted by motion artifact, the self coupling feature is absent. Based on all of these observations, Neyman-Pearson (NP) rules are formulated for each of the measures. It is understood that kurtosis based detection is more reliable than the skew measure. It is also seen that fusing decisions based on individual measures further enhance the overall detection capability. In summary, the HOS based motion detection algorithm is a robust and reliable method to identify corrupt data frames that can be further processed for motion artifact removal.

7. REFERENCES

[1] N. Mammone and F.C Morabito "Independent component analysis and high-order statistics for automatic artifact rejection", *Proceedings of IEEE International Joint Conference on Neural Networks, 2005* IJCNN '05, Volume 4, 31 July-4 Aug. 2005, pp. 2447 - 2452.

[2] B. Pilgram, P. Castiglioni, G. Parati, and M. Di Rienzo, "Dynamic detection of rhythmic oscillations in heart-rate tracings: A state-space approach based on fourth-order cumulants", *Biol. Cyber.,* vol. 76, pp. 299 - 309, 1997.

[3] J. M. Mendel, "Tutorial on Higher-Order Statistics (Spectra) in Signal Processing and System Theory: Theoretical Results and Some Applications", *Proc. IEEE*, vol. 79, pp. 278 - 305, January 1991.

[4] C. L. Nikias and A. P. Petropulu, *Higher-Order Spectra Analysis: A Nonlinear Signal Processing Framework,* Prentice Hall Inc., 1993.

[5] A Swami, J. M. Mendel and C. L. Nikias, *Higher-Order Spectral Analysis Toolbox For Use with MATLAB*, User's Guide Version 2.

[6] C. L. Nikias and M.R. Raghuveer, "Bispectrum Estimation: A digital signal processing framework", *Proc. IEEE,* vol. 75, no.7, pp. 867 - 891, 1987.

[7] A. Mansour and C. Jutten,"What should we say about the kurtosis?", *Signal Processing Letters, IEEE* vol. 6, issue 12, pp. 321 - 322, December 1999.

[8] Jianchu Yao, S. Warren , "A Short Study to Assess the Potential of Independent Component Analysis for Motion Artifact Separation in Wearable Pulse Oximeter Signals", *27th Annual International Conference of the Engineering in Medicine and Biology Society, 2005*, pp. 3585 - 3588, 2005.

[9] R. F. Dwyer, "Use of the Kurtosis Statistic in the Frequency Domain as an Aid in Detecting Random Signals", *IEEE Journal of Oceanic Engineering*, vol. OE-9, No.2, pp. 85 - 92, April 1984.

[10] J. Muthuswamy, D. L. Sherman and N. V. Thakor, "Higher-Order Spectral Analysis of Burst Patterns in EEG", *IEEE Transactions On Biomedical Engineering,*, vol. 46, No. 1, January 1999.

[11] Z. Chair and P. Varshney, "Optimal data fusion in multiple sensor detection systems", *IEEE Transaction Aerospace Electronic Systems, AES*, 22 (Jan) 1986, pp. 98 - 101.

[12] J. Weng, Z. Ye and J. Weng, "An Improved Pre-processing Approach for Photoplethysmographic Signal", *27th Annual International Conference of the Engineering in Medicine and Biology Society, 2005*, IEEE-EMBS 2005, pp. 41 - 44, 01-04 Sept. 2005.